Journal of Drug Delivery Science and Technology 79 (2023) 104085

Contents lists available at ScienceDirect

Journal of Drug Delivery Science and Technology

journal homepage: www.elsevier.com/locate/jddst

Novel cannabinoid release system: Encapsulation of a cannabidiol precursor into γ-cyclodextrin metal-organic frameworks

Jorge Rodríguez-Martínez [1], María-Jesús Sánchez-Martín [*,1], Oscar López-Patarroyo, Manuel Valiente

GTS Research Group, Department of Chemistry, Faculty of Science, Universitat Autònoma de Barcelona, 08193, Bellaterra, Spain

ARTICLE INFO

Keywords:
γ-Cyclodextrin-metal-organic frameworks (γ-CD-MOFs)
Cannabidiol (CBD)
Cannabinoids
Drug delivery systems (DDS)
Olivetol (OLV)

ABSTRACT

γ-Cyclodextrin-metal-organic frameworks (γ-CD-MOFs) are developed as a new promising and biocompatible material, which shows a great potential for drug delivery system (DDS) applications. γ-CD-MOFs were successfully synthesized using microwave-assisted technique from different potassium sources (KOH, KCl and KNO_3). The encapsulation of olivetol (OLV) into these materials was investigated as an innovative model of DDS for cannabinoids. Loading of OLV in γ-CD-MOFs was performed by impregnation and co-crystallization methods. Scanning electron microscopy (SEM) and X-ray powder diffraction (XRPD) were employed to study the structural properties of γ-CD-MOF samples, showing the typical cubic crystals in case of KOH and trigonal morphologies in case of KCl and KNO_3. Olivetol content was determined using UV–Vis spectrophotometry and its interaction with γ-CD-MOFs was investigated by Attenuated Total Reflection-Fourier Transform Infrared Spectroscopy analysis (ATR-FTIR). OLV content was significantly higher when KCl or KNO_3 were employed in combination with a co-crystallization method, while the drug encapsulation using KOH and the impregnation method was really poor. For the first time, γ-CD-MOFs loaded with cannabinoids were developed and they could be considered a novel strategy as DDS of these compounds.

1. Introduction

Metal-organic frameworks (MOFs) have emerged in several applications such as gas storage, catalysis, pollutant-removal agents and drug delivery systems (DDS) [1,2]. These materials are made of metal ions and organic ligands linked in an infinite extended one-two-three dimensional networks [3]. This packing confers crystallinity and extraordinary properties to MOFs such as high surface areas, ultrahigh porosity and thermal stability making them promising for plenty applications as already mentioned above [4]. Moreover, the parameters that define these properties could be modified by the selection of the linkers and the control of the different steps during the synthesis procedure [5]. Another aspect to take into account is the formation of the host-guest complexes. This encapsulation process depends on the drug to encapsulate and on the medium. In fact, there are a lot of methodologies for this purpose, like direct impregnation, vaporization, direct contact pressure or co-crystallization techniques [6]. Furthermore, the procedure should be selected properly in order not to affect the properties of the MOFs.

Within the uses of MOFs, the application of these materials in biomedical field has been growing over the last years since they could act as drug delivery systems in order to improve the characteristics of the encapsulated agent and to target its pharmaceutical effect [7]. Nevertheless, biocompatibility is a key aspect in these cases and the components that comprise the MOFs should show low toxicity [8,9]. In recent years, γ-cyclodextrin-metal-organic frameworks (γ-CD-MOFs) have arisen as promising biocompatible candidates due to their relevance in pharmacy and biomedicine [10]. These types of MOFs are made of γ-cyclodextrin as the organic ligand and the selected metal linker. γ-CD presents a hydrophobic inner cavity where non-polar compounds could be encapsulated and a hydrophilic outer surface allowing its solubility in aqueous solutions [11]. Besides, the encapsulation capacity of γ-CD-MOFs is higher than in the γ-CD alone and, according to reported studies; these MOFs improve the physicochemical and biopharmaceutical characteristics of the encapsulated drug and control its release process [12,13]. In order to perform the synthesis of these materials, the

* Corresponding author.
E-mail address: mariajesus.sanchez@uab.cat (M.-J. Sánchez-Martín).
[1] Shared co-first authorship.

https://doi.org/10.1016/j.jddst.2022.104085
Received 27 May 2022; Received in revised form 7 December 2022; Accepted 12 December 2022
Available online 14 December 2022

vapor diffusion technique is the most conventional and well-known method but it requires at least several days to obtain γ-CD-MOFs [14]. Therefore, new methodologies are being developed in order to solve this difficulty, such as the analytical microwave-assisted technique, obtaining homogeneous crystal structures with editable size and a suitable reaction yield [15,16]. Moreover, the synthesis time has been reduced from days to hours using this technique instead of the vapor diffusion method. Thus, microwave technique emerges as a fast and efficient methodology in the synthesis of these frameworks. CD-MOFs based on α-CD, β-CD or γ-CD using potassium nitrate were developed for menthol encapsulation [17]. The obtained crystals presented uniform size, ordered structures and regular shape, showing a better thermal stability than alone CDs. This study could be useful in the design of efficient materials in the food industry. Moreover, other study has made an attempt to improve the encapsulation of the insoluble drug, honokiol, into the pores of γ-CD-MOFs using supercritical carbon dioxide for its activation [18]. The resulting DDS improved the solubility and bioavailability of the drug and the activation of the MOFs maximized its potential encapsulation capability.

Cannabidiol (CBD) is the main non-psychotropic cannabinoid of the *Cannabis sativa* plant. This compound is the main component responsible of the medical benefits of cannabis. Cannabidiol and other natural cannabinoids act on the endocannabinoid system [19]. This system regulates several physiological processes in the body related to cognition and brain function, pain pathways in the brain, immune and hematopoietic systems. Therefore, CBD presents interesting properties such as its analgesic, anti-inflammatory and immunomodulatory effects [20]. Because of that, this compound has been employed in several studies over the last few years for the treatment of diseases such as Alzheimer or cancer [21,22]. These promising effects in a lot of different diseases are due to the capacity of CBD to interact not only with the corresponding endocannabinoid receptors but also with a wide spectrum of others receptors [23]. However, CBD also presents some limitations that compromise its plenty applications. This compound is insoluble in water, it presents low chemical stability and it gets oxidized in alkali media [24]. Consequently, numerous materials for CBD encapsulation have been developed to minimize these weaknesses, including inclusion complexes of cyclodextrins, lipid carriers and microparticles, among others [25]. Poly (lactic-*co*-glycolic acid) spherical microparticles were used for CBD encapsulation improving the administration of the drug and showing a useful formulation to be combined with conventional chemotherapy against ovarian cancer [26]. In other study, the preparation of stable inclusion complex of CBD with three native cyclodextrins increased significantly the water solubility and *in vitro* anticancer activity of cannabidiol compared with free drug thanks to the encapsulation of the CBD into the inner cavity of cyclodextrins [27]. Similarly, nanostructured lipid carriers formulations loaded with CBD were developed and characterized as a promising delivery system to enhance the bioavailability of cannabidiol for the treatment of neuropathic pain [28]. Even though there are several studies on the encapsulation of cannabidiol into different carriers, investigations on CBD being loaded into γ-CD-MOFs have not been reported. Nevertheless, cannabidiol is not a very affordable product, therefore analogues or precursors of this compound could be used instead of CBD for multiple experimental approaches. Olivetol (OLV), also known as 5-pentylresorcinol, is a natural organic compound found in certain species of plants [29] and itis an intermediate involved in the cannabinoid biosynthesis in *C. sativa.* This compound leads to the different cannabinoids, including CBD becoming an important metabolite in cannabinoid biosynthesis [30]. In fact, it is used in various methods to produce synthetic analogues of cannabinoids [31]. Chemically, OLV structure is found in cannabinoids, so OLV could be used as an analogue of CBD as it could mimic its interactions with the drug delivery systems.

The aim of this study is to develop CD-MOFs for olivetol encapsulation as a model of cannabinoid drug delivery system. CD-MOFs are prepared using γ-CD and three different potassium sources depending on the followed synthesis method. The characterization of the drug delivery systems is performed and the encapsulation efficiency of OLV into γ-CD-MOFs is determined. For the first time, γ-CD-MOFs are used for olivetol encapsulation, and it could be useful in the development of CD-MOFs as promising drug delivery systems with analgesic effect in pharmacy and biomedical field.

2. Materials and methods

2.1. Reagents

Olivetol (95%) and γ-cyclodextrin (98%) were purchased from Carbosynth Ltd (Compton, United Kingdom). Potassium hydroxide (85.5%) and potassium nitrate (99.2%) were purchased from VWR BDH Chemicals (Oud-Heverlee, Belgium). Dichloromethane (99.5%) and ethanol (96%) were purchased from Scharlau (Sentmenat, Spain). Potassium chloride (99.0%) was purchased from Sigma-Aldrich (St. Louis, MO, USA). Polyethylene glycol 20,000 was purchased from Merk (Darmstadt, Germany). Methanol (99.8%) and acetic acid (99.9%) were purchased from Fisher Scientific (Madrid, Spain). MilliQ water was purified through a Millipore purification system from Millipore (Milford, MA, USA).

2.2. Preparation of the samples

A fast synthesis of γ-CD-MOFs with microwave irradiation was performed using a modified method [1]. This reported method offers the advantages of simple, rapid, inexpensive, relatively green, and efficient non-conventional heating and high yield [13]. Briefly, γ-CD (324 mg) and KOH (112 mg) were mixed in milliQ water (10 mL). The molar ratio of KOH to γ-CD was 1:8. Then, 6 mL of methanol were added. This initial solution was treated at 50 °C in the analytical microwave (CEM Corporation Matthews, North Carolina, USA) for 10 min and a power of 600 w. After that process, 256 mg of PEG 20000 were added for 1 h to trigger the precipitation of the crystals at room temperature. In order to remove the unreacted material, the crystals were washed first with 10 mL of methanol and then with 10 mL more of ethanol in a centrifuge at 3000 rpm for 5 min. Next, γ-CD-MOFs were left under vacuum and dried overnight at 50 °C. Herein, preliminary alkaline γ-CD-MOFs (pH = 12) were obtained. Since cannabinoids get oxidized in alkali media, a neutralization of the γ-CD-MOFs was needed. For this step, the crystals were treated with a mixture of 5.2 mL of ethanol and 0.8 mL of acetic acid. The suspension was then shaken at 290 rpm for 2 h and the precipitates were collected by centrifugation (3000 rpm for 5 min). Once again, the powder was left to dry overnight under vacuum at 50 °C. Afterwards, an activation of the γ-CD-MOFs was performed using a solvent exchange method with dichloromethane in order to remove guest molecules from chemicals used in the synthetic procedure. γ-CD-MOFs were mixed with 10 mL of dichloromethane at 290 rpm for 3 days. Every 24 h the solvent was replaced by centrifugation (3000 rpm for 5 min). Finally, the samples were dried overnight under vacuum at 50 °C. γ-CD-MOFs were kept under vacuum at room temperature until its use and the reaction yields were also calculated.

Impregnation and co-crystallization methods were performed to load olivetol into γ-CD-MOFs. In case of impregnation, 30.8 mg of MOF samples were added to 20 mL of OLV 360 mg/mL solution in ethanol in order to obtain a 1:2 M ratio of γ-CD-MOFs:OLV respectively. The suspensions were incubated for 24 h at 37 °C under stirring conditions (290 rpm). After the incubation time, the crystals were washed with 10 mL of ethanol in a centrifuge at 3000 rpm for 5 min in order to remove the drug that did not interact with the γ-CD-MOFs. Finally, the samples were dried and kept under vacuum at room temperature until its use.

The co-crystallization method is similar to that described before. In this case, the potassium sources were KCl or KNO_3 instead of KOH, adding 149 mg or 202 mg respectively, to maintain the 1:2 M ratio. The change in the potassium source is because of in the co-crystallization the

drug is loaded on the initial solution where the synthesis takes place, and the pH of the medium must be neutral from the beginning to avoid olivetol oxidation. Additionally, 30 mg of OLV were also diluted in the initial solution. This amount of drug was selected in order to keep the same molar ratio between MOF and olivetol as in the impregnation method. In this method, the incubation time with PEG 20000 was 24 h instead of 1 h in order to maintain the same incubation time with OLV for its encapsulation as in the impregnation method, thus making them comparable but the neutralization and activation steps were not needed. Finally, the washes were the same as before and the resultant samples were left overnight under vacuum at 50 °C and kept under vacuum at room temperature until its use. It should be noted that MOFs were not obtained when KCl or KNO_3 were employed following the same synthesis procedure as for KOH.

The γ-CD-MOFs loaded by impregnation method was named as γ-CD-MOF-1, loaded or not with OLV. In the case of co-crystallization technique, MOFs were named as γ-CD-MOF-2 and γ-CD-MOF-3, for KCl and KNO_3 as potassium sources respectively.

2.3. Drug release and quantification

The quantification of the drug encapsulation into the MOFs was determined as follows: 15 mg of MOF sample were added to 5 mL of a mixture of milliQ water and ethanol (1:1, v/v). The mixture was incubated at room temperature under stirring conditions (290 rpm) for 24 h to promote the degradation of the crystals and release the encapsulated OLV. To determine the amount of olivetol, the solution was measured by UV–Vis spectrophotometry (Thermo Fisher Scientific, Massachusetts, USA) [32]. The UV detection was performed at 275 nm that is the characteristic peak of OLV and the reference was a mixture of milliQ water and ethanol (1:1, v/v). A calibration curve of different known concentrations of olivetol in milliQ water and ethanol solutions (1:1, v/v) was also performed from 0 to 100 mg/L of the drug (Fig. A.1) to determine the concentration of olivetol in the samples.

The drug loading for each MOF was calculated following equation (1):

$$Drug\ loading\ (\%) = \frac{Encapsulated\ OLV\ into\ CD-MOFs\ (mg)}{Total\ Weight\ of\ coplexation\ powder\ (mg)} \cdot 100 \qquad [1]$$

All determinations of the loaded drug in each MOF sample were performed by triplicate.

2.4. Scanning electron microscope and energy-dispersive X-ray spectroscopy

The morphology and elemental composition of the MOF samples were analysed by Scanning Electron Microscopy (SEM) and Energy Dispersive X-ray Spectroscopy (EDX) with a Zeiss Merlin FE-SEM equipped with an EDX Oxford INCA X-Max Detector. The images were taken with the Secondary Electron Detector with a low voltage of 1–2 kV and the EDX measurements were taken at 10 kV. This microscope has a unique charge compensation system that allows the high-resolution imaging of non-conductive samples, electrons which accumulate on the sample surface are swept away by a fine jet of nitrogen. All the experiments were performed at room temperature.

2.5. X-ray powder diffraction analysis

The crystallinity of the MOFs samples was characterized by X-ray powder diffraction (XRPD) using a Malvern Panalytical X'Pert PRO MPD (Material Powder Diffractometer). The MPD is suitable for the analysis of polycrystalline samples at room temperature. This diffractometer has a vertical theta-theta goniometer (240 mm radius). The XRD analysis was carried in transmission mode using a capillary spinner and the sample were filled inside borosilicate glass capillaries with outer diameter of 0.7 mm. A focusing mirror was used for the incident beam and a lineal X'Celerator detector for the diffracted beam. The samples were irradiated with a ceramic X-ray tube with Cu Kα anode (l = 1.5406 Å), tube voltage of 45 kV, tube current of 40 mA in a step size scan mode (0.03° min^{-1}) and analysed over a 2θ angle range of 2.5–35°.

2.6. Attenuated total reflection-fourier transform Infrared Spectroscopy analysis

Infrared Spectroscopy spectra of samples were obtained using an Infrared Spectrophotometer Tensor 27 equipped with an Attenuated Total Reflectance module Specac Golden Gate (ATR-FTIR, Bruker, Ettlingen, Germany). The ATR accessory allows direct recording of samples thus facilitating the recording of IR spectra on liquid or solid samples regardless of their physical nature. To measure the powder samples 64 scans were carried out in wavenumber from 4000 cm^{-1} to 600 cm^{-1} at a resolution of 4 cm^{-1} and at room temperature. For the background the own diamond window of the equipment was used.

3. Results and discussion

3.1. Structural properties of γ-CD-MOFs

The crystal morphology and element distribution of different γ-CD-MOFs compared with native γ-CD were determined by SEM and EDX analysis. In case of γ-CD-MOF-1, the final morphology of the crystals matched very well with the previously reported morphology of the same material (Fig. 1A) [10]. The SEM images of γ-CD-MOF-1 showed that they presented cubic-shaped with a size average of 2 μm, while the morphology of the raw γ-CD alone was completely amorphous when the same technique was performed (Fig. A.2). Moreover, the EDX detector in the SEM equipment was used to the elemental qualitative analysis of γ-CD-MOF-1 and it confirmed the presence of potassium in the cubic structures (Table A.1). Thus, the cubic crystals were the material of interest. Furthermore, the size average of the structures was reduced in comparison with the γ-CD-MOFs obtained with conventional methodologies, such as vapor diffusion method (Fig. A.3). This fact demonstrated the high capabilities of the microwave technique to achieve narrow size distributions and control of the morphology in the MOFs synthesis. Indeed, this is a key point when the final application of the structures is as drug delivery systems. In the case of olivetol loaded γ-CD-MOF-1, similar size and cubic shape were observed in comparison with the unloaded ones (Fig. 1B). Therefore, the morphology of the MOF structures was stable after the encapsulation with the drug. In case of γ-CD-MOF-2 and γ-CD-MOF-3, the resultant crystals presented a different morphology when they were compared with γ-CD-MOF-1 and the reported ones. Co-crystallization of γ-CD-MOFs with OLV showed a rectangular shape as elongated prims and a bigger and less homogeneous size than in the synthesis with KOH. The differences in size and homogeneity may be due to the incubation time with PEG during the synthesis process [1]. Since in γ-CD-MOF-1 the incubation time was 1 h, in the co-crystallization it took 24 h to get the precipitation of the crystals. It was reported that if enough amount of time is allowed for crystallization, larger particles will obtain but also small ones because synthesis during a short time may be also possible. Therefore, the size will not be homogeneous and bigger crystals will be obtained [15]. Differences observed in shape between MOFs obtained by co-crystallization (γ-CD-MOF-2 and γ-CD-MOF-3) and γ-CD-MOF-1 may be due to the use of the potassium salts instead of KOH as metal source. The change of this reagent modifies an important solution parameter such as pH. For γ-CD-MOF-1, the pH of the initial solution was 12 and in the co-crystallization the pH was 7. It is reported that the pH control of the environment of the reaction medium in MOFs synthesis allows you to control the size and the morphology of the resulting crystals [33]. Moreover, the totality of studies that synthetize γ-CD-MOF use alkali media in order to get the classic cubic shapes regardless of metal source. The fact that both KCl and KNO_3 led the same elongated prisms

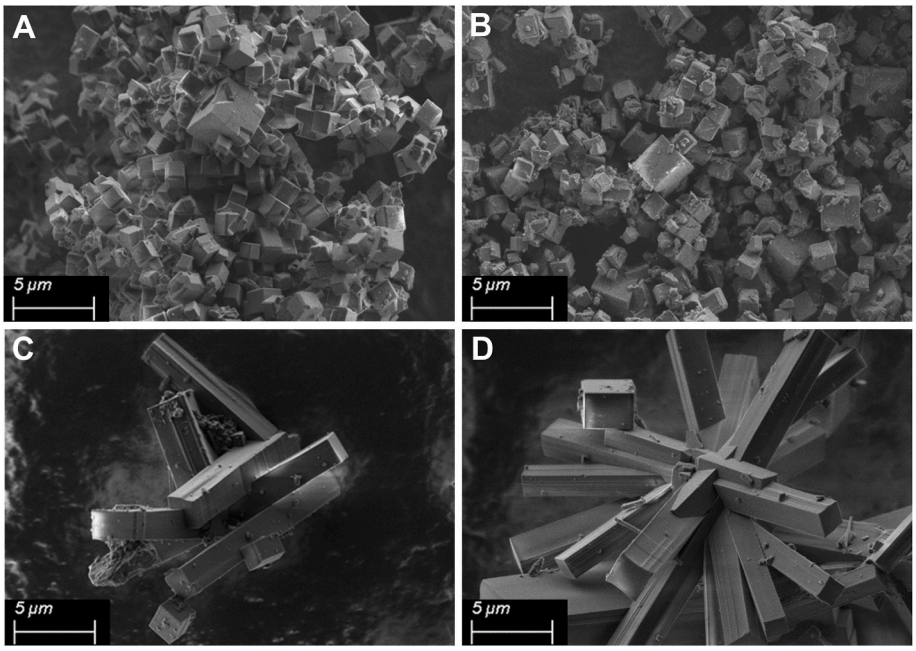

Fig. 1. Scanning electron microscopy images of unloaded γ-CD-MOF-1 (A), olivetol loaded γ-CD-MOF-1 (B), γ-CD-MOF-2 (C) and γ-CD-MOF-3 (D) with a low voltage of 2 kV, 5000x of magnification and a working distance of 4.7 mm.

morphologies supports this pH-dependent theory. Besides that, EDX analysis also showed the presence of potassium in the MOFs obtained by co-crystallization (Table A.1), confirming the interaction between the metal ion and the organic ligand to form this material.

Further characterization was performed using X-ray diffraction. The crystallinity of γ-CD-MOF-1 before and after the encapsulation experiments with the drug was measured by XRPD. According to reported studies about the synthesis of γ-CD-MOFs using KOH, the characteristic peaks in X-ray diffraction patterns of these materials are located in the next angles: 4°, 5.7°, 7°, 13.3° and 16.6°. These positions correspond to body-centered cubic crystals of space group *I*432 [34]. XRPD results showed that the diffractogram of the unloaded MOFs presented the same peaks in comparison with the standard reference of these crystals (Fig. 2 and fig. A.4). Therefore, the crystalline phase obtained for γ-CD-MOF-1 coincided with the typical cubic unit of these materials. Comparing the data before and after the encapsulation experiment with olivetol, the crystallinity of MOFs loaded with the drug changed with respect to the unloaded crystals. The intensity of the peaks of the γ-CD-MOF-1 with OLV was significantly reduced compared to those of the unloaded MOFs (Fig. 2). This partial loss of crystallinity of the MOFs may result from the filling of pores with olivetol, the high degree of disorder of the drug and the presence of a low percentage of water in the ethanol solution used in these experiments [32]. However, the peak positions in the diffractograms were similar in both cases indicating that MOF crystals were stable after the encapsulation with olivetol [35]. Moreover, no new diffraction peaks appeared into the olivetol loaded MOFs, suggesting that the encapsulated drug is in an amorphous state. Taking into account SEM and XRPD results, we can conclude that the morphology of the γ-CD-MOF-1 was stable after the encapsulation with the drug, in spite of the partial loss of crystallinity. For γ-CD-MOF-2 and γ-CD-MOF-3, important changes were observed in the diffraction patterns (Fig. 2). The partial loss of crystallinity was observed again in the co-crystallization MOFs with a similar intensity in the diffraction peaks as in the previous case of OLV loaded γ-CD-MOF-1, probably due to the encapsulation of the drug. Furthermore, the characteristics positions peaks were located in different angles: 5.3°, 7.4°, 10.5°, 11.5°, 12.1°, 14.2°, 14.9°, 15.8° and 16.7°. These peaks did not correspond with the diffraction pattern described before for the conventional CD-MOFs synthetized with KOH, despite the metal linker has not changed. Moreover, they did not

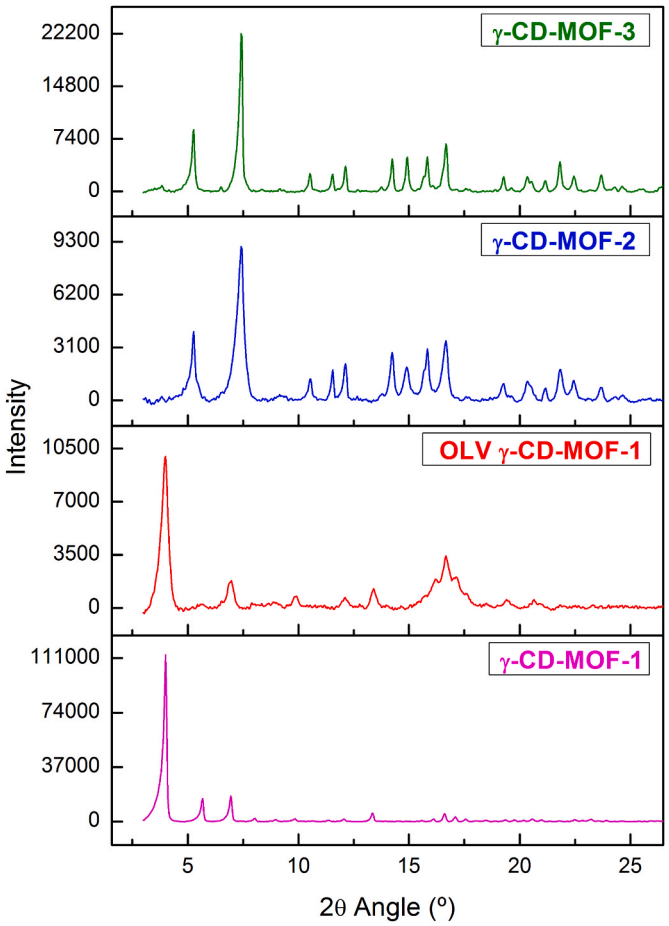

Fig. 2. X-ray powder diffraction patterns of unloaded γ-CD-MOF-1 (pink), olivetol loaded γ-CD-MOF-1 (red), γ-CD-MOF-2 (blue) and γ-CD-MOF-3 (green). (For interpretation of the references to colour in this figure legend, the reader is referred to the Web version of this article.)

match with the peaks of raw γ-CD or any simulated references (Fig. A.4). A possible explanation for that is the pH of the initial solution during the MOF synthesis, as described before for SEM results. Since for γ-CD-MOF-1 the pH of the initial solution was around 12 due to the use of potassium hydroxide, for γ-CD-MOF-2 and γ-CD-MOF-3 the potassium salts led the initial solution to a neutral pH. It is reported that the body-centered cubic CD-MOFs were grown from solutions of basic salts, such as hydroxides and carbonates. Although this alkali media is not enough to deprotonate the hydroxyl groups of γ-CD, it seems to facilitate the growing of this type of crystals [36]. Moreover, previous studies about CD-MOFs have reported trigonal crystals with several spaces groups (*R*32, *I*4, *P*1 or $P3_2$) different from *I*432 [5,36]. In these CD-MOFs, the metal sources were not the typical potassium hydroxide. Therefore, the metal linker and the pH of the initial solution could be causes of the different morphology and diffraction pattern observed for the CD-MOFs. This fact would explain the new diffraction patterns in γ-CD-MOF-2 and γ-CD-MOF-3 that did not match with the cubic space group *I*432 correlating to the trigonal morphology observed in their respective SEM images.

3.2. Reaction synthesis yield and olivetol content in γ-CD-MOFs

Reaction time, power and temperature were selected according to bibliography [1]. Reaction time was critical in the fabrication of these MOFs crystals due to the crystallization kinetics such as nucleation. They are time dependent factors and if the time is too short, the development of the crystallization process cannot occur, and the yield is too small. However, a dramatic loss in crystallinity has been reported for prolonged reaction time in previous studies [47]. Thus, a reasonable reaction time value should be employed to be able to obtain enough yield without compromise the structural properties of the samples. Power and temperature are also crucial in the yield of the MOFs, since increasing these factors the solution is keeping away from the supersaturation and the crystallization process does not occur. The opposite effect is observed if the temperature and power are too low, the rapid oversaturation of the reagents in the initial solution takes place and the crystal formation cannot happen. In the synthesis process of the γ-CD-MOF-1 using KOH, the reaction yield matched well with the values described in reported studies [13,37]. Nevertheless, in co-crystallization syntheses (γ-CD-MOF-2 and γ-CD-MOF-3) similar reaction yields were obtained but much lower than for the γ-CD-MOF-1 (Table 1). These differences are due to the pH change, as typical cubic CD-MOFs growing is favoured in alkali solutions [36]. As it was reported in the previous section, γ-CD-MOF-2 and γ-CD-MOF-3 presented different morphology and diffraction pattern, so the kinetics for the precipitation of the crystals should not be the same as for the γ-CD-MOF-1 crystal formation because of the different pH values due to the alternative potassium sources. In fact, this could also explain the absence of MOFs using KCl or KNO_3 but following the procedure of conventional synthesis with KOH.

Not only reaction yields have changed depending on the potassium source but also the drug loading content (Fig. 3). For OLV γ-CD-MOF-1 the drug content was really poor using the impregnation method to perform the encapsulation. This could be explained due to the hybrid polarity behaviour of OLV. Olivetol dissolves perfectly in organic solvents but it is partially miscible in aqueous solutions. According to that, OLV would tend to be more comfortable on a hydrophobic environment like the inner cavities of the MOFs, than in the ethanol solution used for the encapsulation that is a relatively polar organic solvent. However, this hybrid polarity behaviour may cause that olivetol could interact with both hydrophobic and hydrophilic environments and the drug is not strongly attracted to the inner cavities of the MOFs, affecting its encapsulation efficiency. In the case of the co-crystallization process, the drug loading was higher than the impregnation method, showing γ-CD-MOF-2 slightly more OLV content than γ-CD-MOF-3 (Fig. 3). This efficiency in the co-crystallization could be explained by the formation of crystals itself. γ-CD-MOF-2 and γ-CD-MOF-3 precipitation may directly trap the drug into the MOF cavities, regardless the hybrid polarity behaviour of OLV. Moreover, drug loading values of co-crystallization synthesis were in agreement with reported studies about γ-CD-MOFs obtaining encapsulation percentages from 2% to 10% for different compounds [12,17,38]. However, this factor could be optimized modulating different parameters such as incubation temperature and time, methanol content in the initial solution and the olivetol amount used during the encapsulation process.

Table 1
Reaction synthesis yield of γ-CD-MOF-1, γ-CD-MOF-2 and γ-CD-MOF-3 with their respective standard deviations.

MOF sample	Reaction yield (%)	σ
γ-CD-MOF-1	59.44	0.03
γ-CD-MOF-2	30.98	0.06
γ-CD-MOF-3	34.65	0.04

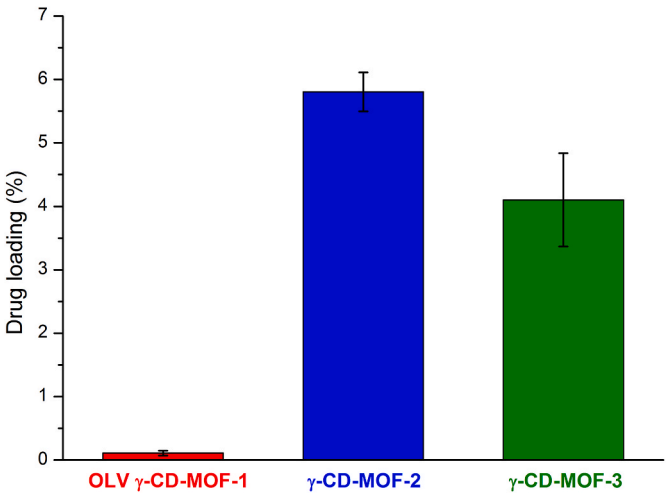

Fig. 3. Drug loading percentage of olivetol in γ-CD-MOF-1, γ-CD-MOF-2 and γ-CD-MOF-3 with their respective standard deviations.

3.3. Characterization of γ-CD-MOFs and olivetol interaction: ATR-FTIR analysis

FTIR spectroscopy is a useful tool to detect the bonding changes between functional groups of the MOFs, the drug and the resulting interactions of both components. There were characteristic peaks in all γ-CD-MOF samples at 1078 cm^{-1}, 1152 cm^{-1}, 1336 cm^{-1}, 2700–2995 cm^{-1} and 3000–3670 cm^{-1} (Fig. 4A). These peaks were in agreement with previous reported literature of γ-CD-MOFs [10,39–41]. Moreover, these regions in the MOF spectra also coincided with the characteristic peaks in the γ-CD spectrum, showing the presence of the organic linker in the crystals. At 1078 cm^{-1}, an antisymmetric stretching vibration mode derived from the C–O–C groups in aliphatic ethers can be observed. These ether groups are presented in the γ-CD structure. The units of γ-CD are α-*d*-glucopyranose molecules with intra-monomeric ether bonds 1 → 5. These units are linked to each other through inter-monomeric ether bonds 1 → 4. The peak at 1152 cm^{-1} was assigned to the stretching vibration between carbon and oxygen atoms in C–OH groups of the two secondary alcohols that are in each unit of α-*d*-glucopyranose. The peak at 1336 cm^{-1} was related to the contribution of alkane groups and the band from 2700 to 2995 cm^{-1} were the contributions of the C–H antisymmetric and symmetric stretching vibrations of CH_2 and CH_3 in aliphatic compounds. These regions may come from the CH_2 group in the hydroxymethyl side chain in each α-*d*-glucopyranose unit of γ-CD. A wide band ranging from 3000 to 3670 cm^{-1} was assigned to stretching vibrations of the hydroxyl groups, the

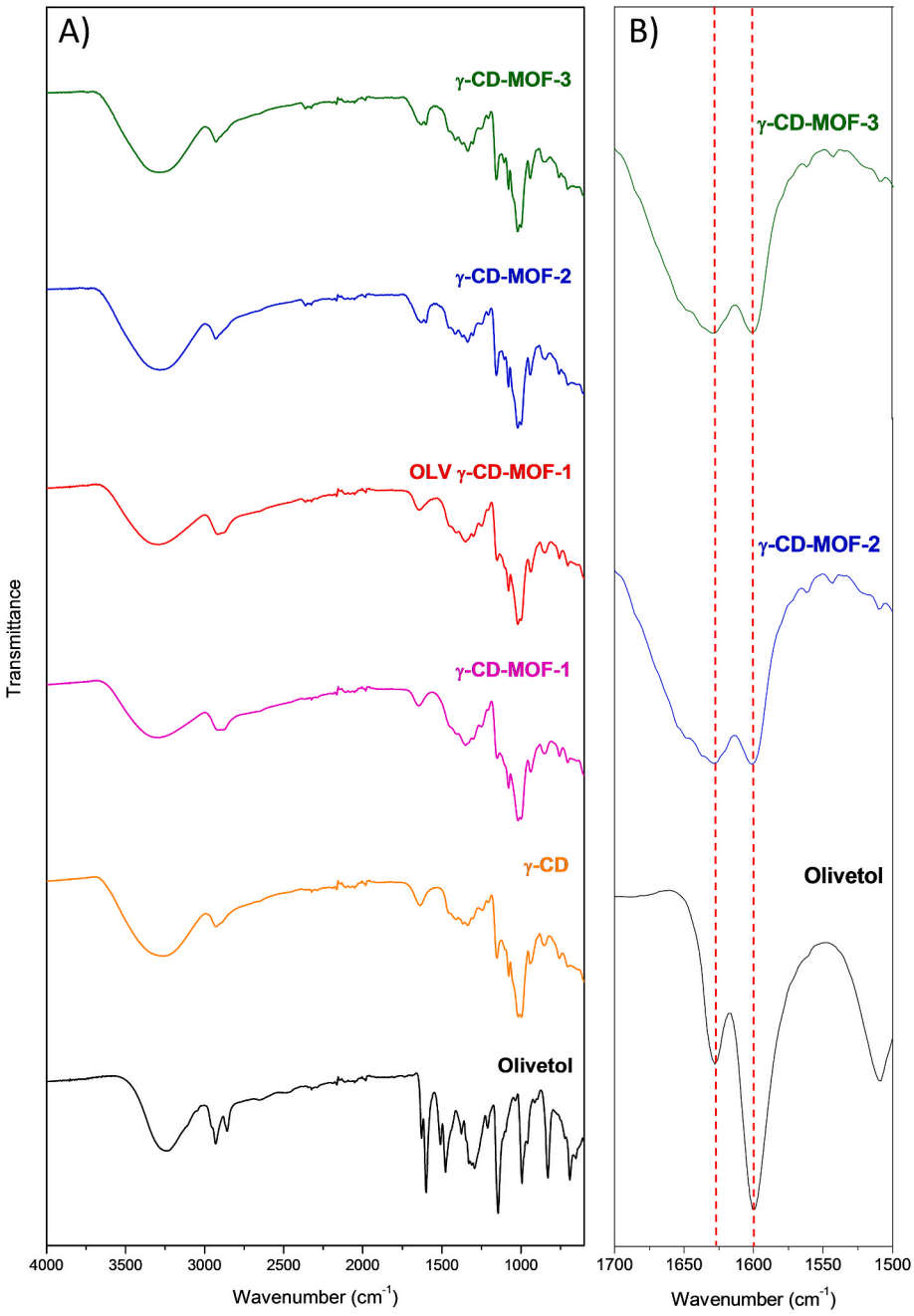

Fig. 4. Attenuated Total Reflection-Fourier Transform Infrared Spectroscopy spectra of: olivetol (black), γ-CD (orange), unloaded γ-CD-MOF-1 (pink), olivetol loaded γ-CD-MOF-1 (red), γ-CD-MOF-2 (blue) and γ-CD-MOF-3 (green) from 4000 cm^{-1} to 600 cm^{-1} (A). Magnified comparison of olivetol (black), γ-CD-MOF-2 (blue) and γ-CD-MOF-3 (green) spectra (B) in the region of interest from 1700 cm^{-1} to 1500 cm^{-1} marking the double peak at 1600 and 1628 cm^{-1}. (For interpretation of the references to colour in this figure legend, the reader is referred to the Web version of this article.)

ones that are secondary alcohols groups but also the primary alcohol in the hydroxymethyl side chain in each α-*d*-glucopyranose unit. In addition to these characteristic bands of γ-CD-MOFs, the peak observed at 1640 cm^{-1} may be due to the hydroxyl groups of water molecules that still remained into the cavities of the MOFs after the drying process. The spectrum of olivetol showed the characteristic peaks of this drug according to the literature at 690 cm^{-1}, 830 cm^{-1}, 1145 cm^{-1}, 1210 cm^{-1}, 1310 cm^{-1}, 1376 cm^{-1}, 1477 cm^{-1}, 1600 cm^{-1}, 1628 cm^{-1}, 2858 cm^{-1}, 2929 cm^{-1} and 3240 cm^{-1} (Fig. 4A) [42–44]. At 690 cm^{-1} and 830 cm^{-1} wavenumbers, two peaks from CH out of plane deformations were observed because of the triple substitution in one, three and five carbon positions in the benzene ring of the OLV. The four peaks at 1145 cm^{-1}, 1210 cm^{-1}, 1310 cm^{-1} and 1376 cm^{-1} corresponded to the stretching vibrations between the carbon and oxygen atoms of the two C–OH groups that are presented in the drug molecule. Moreover, phenols absorb near 1350 cm^{-1} due to the OH deformation and give a second band due to C–OH stretching near 1210 cm^{-1}, and in this case, the two hydroxyl groups are in the benzene ring of the drug. At 1477 cm^{-1} and the double peak at 1600 and 1628 cm^{-1}, two regions of stretching vibrations derived from the interactions between the carbon atoms in the aromatic ring of the olivetol structure and the skeletal stretching vibration of –C═C- could be observed. The peaks at 2858 cm^{-1} and 2929 cm^{-1} were related to the antisymmetric stretching vibrations of C–H bond of CH_2 and CH_3 groups that are presented in the pentyl chain of the molecule. The wide peak at 3240 cm^{-1} was assigned to stretching vibrations between oxygen and hydrogen atoms of the two hydroxyls groups in the aromatic ring. A direct comparison between the infrared spectra of OLV and γ-CD-MOF-1 before and after the encapsulation process with the drug did not show any differences (Fig. 4A). This could be due to the poor encapsulation of the drug in γ-CD-MOF-1 that it was not enough to observe perceptible changes. Nevertheless, γ-CD-MOF-2 and γ-CD-MOF-3 spectra showed in the peak at 1640 cm^{-1} a double peak

at 1600 and 1628 cm^{-1} corresponding to the skeletal stretching –C═C- vibration of OLV (Fig. 4B). It was observed that the 1640 cm^{-1} peak in MOFs is partially occluded by this OLV signal. These results confirmed the interaction between γ-CD-MOFs and olivetol in the co-crystallization, because if this interaction did not take place, OLV would have been removed during the washing steps with the organic solvents. Moreover, this interaction in γ-CD-MOF-2 and γ-CD-MOF-3 was in agreement with the quantification of the drug explained before, that showed a high OLV encapsulation in the co-crystallization samples. In accordance with previous literature, the interaction between OLV and γ-CD-MOFs may take place through the two phenolic hydroxyl groups of the olivetol structure and the inner cavity of the γ-CD molecules. It has been described that cyclodextrin molecules provide their cavities as a non-polar field, in which OLV is complexed through its hydroxyl groups and non-covalent interactions [45]. Furthermore, a study that encapsulates curcumin in γ-CD-MOFs to improve the stability of this compound concluded that the interaction between curcumin and the MOFs is through the phenolic hydroxyl group of the curcumin [46]. Therefore, based on the infrared results of this investigation and previous reported studies, the interactions between olivetol and γ-CD-MOFs may be due to van der Waals forces and hydrophobic effects between the different atoms of the olivetol structure and the inner parts of the non-polar MOF cavities, since shifts on wavenumbers are due to changes on vibrations through the molecules involved and there were not significant shifts in the spectra [45].

4. Conclusions

The present work shows that MOFs based on γ-cyclodextrin and potassium ions serve as an effective drug delivery system of olivetol. OLV was used as a guest model compound of cannabinoids for its encapsulation into these CD-MOFs using impregnation and co-crystallization methods. Microwave technique was used to get a fast synthesis using different potassium sources such as the conventional KOH, as well as KCl and KNO_3 as innovative approach.

SEM and PXRD analysis revealed a trigonal morphology and a different diffraction pattern when the alternative potassium compounds were employed, in comparison with the typical cubic structures obtained with KOH. This fact could be explained due to the different pH of the initial solutions. It was demonstrated that olivetol could be loaded into these carriers by co-crystallization method, solving the problem of its poor encapsulation when the impregnation method was performed. FTIR analysis corroborated the success of this encapsulation. Therefore, the combination of alternative potassium sources and the co-crystallization process resulted in γ-CD-MOFs with a strong potential as drug carriers for cannabinoids compounds, including CBD. Moreover, these materials may become alternative drug delivery systems of unstable molecules in an alkaline or acid solution. Nevertheless, further studies would be convenient to optimize the different crystal precipitation parameters during the co-crystallization process in order to obtain suitable materials for biomedical applications. Cyclodextrin-based MOFs (CD-MOFs) are considered environmentally friendly and biocompatible MOFs. The biocompatibility of γ-CD-MOF was excellent since cyclodextrin was widely used in drug delivery and proven to be safe. However, crystalline stability needs to be evaluated as a fundamental requirement of a potential vehicle for drug delivery, thus, further studies are needed regarding this point.

Author statement

Jorge Rodríguez-Martínez: Conceptualization, Formal analysis, Investigation, Writing - Original, Draft, Writing - Review & Editing, Visualization. María-Jesús Sánchez-Martín: Conceptualization, Writing - Review & Editing, Supervision, Project administration. Oscar López-Patarroyo: Formal analysis, Investigation. Manuel Valiente: Conceptualization, Resources, Writing - Review & Editing, Supervision, Project administration, Funding acquisition.

Declaration of competing interest

The authors declare that they have no known competing financial interests or personal relationships that could have appeared to influence the work reported in this paper.

Data availability

Data will be made available on request.

Acknowledgments

The Spanish Ministerio de Economía y Competitividad is acknowledged for the financial support provided (Project: CTM2015-65414-C2-1-R). Jorge Rodríguez-Martínez acknowledges Agència de Gestió d'Ajuts Universitaris i de Recerca from Generalitat de Catalunya (Sapin) for the FI-2018 fellowship.

Appendix A. Supplementary data

Supplementary data to this article can be found online at https://doi.org/10.1016/j.jddst.2022.104085.

References

[1] B. Liu, Y. He, L. Han, V. Singh, X. Xu, T. Guo, F. Meng, X. Xu, P. York, Z. Liu, J. Zhang, Microwave-assisted rapid synthesis of γ-cyclodextrin metal-organic frameworks for size control and efficient drug loading, Cryst. Growth Des. 17 (2017) 1654–1660, https://doi.org/10.1021/acs.cgd.6b01658.
[2] P. Raju, K. Balakrishnan, M. Mishra, T. Ramasamy, S. Natarajan, Fabrication of pH responsive FU@Eu-MOF nanoscale metal organic frameworks for lung cancer therapy, J. Drug Deliv. Sci. Technol. 70 (2022), 103223, https://doi.org/10.1016/J.JDDST.2022.103223.
[3] B. Liu, H. Li, X. Xu, X. Li, N. Lv, V. Singh, J.F. Stoddart, P. York, X. Xu, R. Gref, J. Zhang, Optimized synthesis and crystalline stability of γ-cyclodextrin metal-organic frameworks for drug adsorption, Int. J. Pharm. 514 (2016) 212–219, https://doi.org/10.1016/j.ijpharm.2016.09.029.
[4] H. Cai, Y.L. Huang, D. Li, Biological metal–organic frameworks: structures, host–guest chemistry and bio-applications, Coord. Chem. Rev. (2019), https://doi.org/10.1016/j.ccr.2017.12.003.
[5] R.A. Smaldone, R.S. Forgan, H. Furukawa, J.J. Gassensmith, A.M.Z. Slawin, O. M. Yaghi, J.F. Stoddart, Metalorganic frameworks from edible natural products, Angew. Chem. Int. Ed. 49 (2010) 8630–8634, https://doi.org/10.1002/anie.201002343.
[6] I. Kritskiy, T. Volkova, A. Surov, I. Terekhova, γ-Cyclodextrin-metal organic frameworks as efficient microcontainers for encapsulation of leflunomide and acceleration of its transformation into teriflunomide, Carbohydr. Polym. 216 (2019) 224–230, https://doi.org/10.1016/j.carbpol.2019.04.037.
[7] Y. Sun, L. Zheng, Y. Yang, X. Qian, T. Fu, X. Li, Z. Yang, H. Yan, C. Cui, W. Tan, Metal–organic framework nanocarriers for drug delivery in biomedical applications, Nano-Micro Lett. 12 (2020) 1–29, https://doi.org/10.1007/s40820-020-00423-3.
[8] V.P. Torchilin, Multifunctional nanocarriers, Adv. Drug Deliv. Rev. 58 (2006) 1532–1555, https://doi.org/10.1016/j.addr.2006.09.009.
[9] X. Unamuno, E. Imbuluzqueta, F. Salles, P. Horcajada, M.J. Blanco-Prieto, Biocompatible porous metal-organic framework nanoparticles based on Fe or Zr for gentamicin vectorization, Eur. J. Pharm. Biopharm. 132 (2018) 11–18, https://doi.org/10.1016/J.EJPB.2018.08.013.
[10] M.P. Abuçafy, B.L. Caetano, B.G. Chiari-Andréo, B. Fonseca-Santos, A.M. do Santos, M. Chorilli, L.A. Chiavacci, Supramolecular cyclodextrin-based metal-organic frameworks as efficient carrier for anti-inflammatory drugs, Eur. J. Pharm. Biopharm. (2018), https://doi.org/10.1016/j.ejpb.2018.02.009.
[11] A.R. Khan, P. Forgo, K.J. Stine, V.T. D'Souza, Methods for selective modifications of cyclodextrins, Chem. Rev. 98 (1998) 1977–1996, https://doi.org/10.1021/cr970012b.
[12] Y. Chen, K. Tai, P. Ma, J. Su, W. Dong, Y. Gao, L. Mao, J. Liu, F. Yuan, Novel γ-cyclodextrin-metal–organic frameworks for encapsulation of curcumin with improved loading capacity, physicochemical stability and controlled release properties, Food Chem. 347 (2021), https://doi.org/10.1016/j.foodchem.2020.128978.
[13] Y. Han, W. Liu, J. Huang, S. Qiu, H. Zhong, D. Liu, J. Liu, Cyclodextrin-Based Metal-Organic Frameworks (CD-MOFs) in Pharmaceutics and Biomedicine, Pharmaceutics, 2018, https://doi.org/10.3390/pharmaceutics10040271.
[14] J. Qiu, X. Li, R. Gref, A. Vargas-Berenguel, Carbohydrates in Metal Organic Frameworks: Supramolecular Assembly and Surface Modification for Biomedical

Applications, Elsevier Inc., 2020, https://doi.org/10.1016/b978-0-12-816984-1.00022-6.
[15] N.A. Khan, S.H. Jhung, Synthesis of metal-organic frameworks (MOFs) with microwave or ultrasound: rapid reaction, phase-selectivity, and size reduction, Coord. Chem. Rev. 285 (2015) 11–23, https://doi.org/10.1016/j.ccr.2014.10.008.
[16] K. Pintado-Palomino, O. Peitl Filho, E.D. Zanotto, C. Tirapelli, A clinical, randomized, controlled study on the use of desensitizing agents during tooth bleaching, J. Dent. 43 (2015) 1099–1105, https://doi.org/10.1016/J.JDENT.2015.07.002.
[17] Z. Hu, S. Li, S. Wang, B. Zhang, Q. Huang, Encapsulation of menthol into cyclodextrin metal-organic frameworks: preparation, structure characterization and evaluation of complexing capacity, Food Chem. 338 (2021), 127839, https://doi.org/10.1016/j.foodchem.2020.127839.
[18] Y. He, X. Hou, J. Guo, Z. He, T. Guo, Y. Liu, Y. Zhang, J. Zhang, N. Feng, Activation of a gamma–cyclodextrin–based metal–organic framework using supercritical carbon dioxide for high–efficient delivery of honokiol, Carbohydr. Polym. 235 (2020), 115935, https://doi.org/10.1016/j.carbpol.2020.115935.
[19] N. Noreen, F. Muhammad, B. Akhtar, F. Azam, M.I. Anwar, Is cannabidiol a promising substance for new drug development? A review of its potential therapeutic applications, Crit. Rev. Eukaryot. Gene Expr. 28 (2018) 73–86, https://doi.org/10.1615/CritRevEukaryotGeneExpr.2018021528.
[20] S. Atalay, I. Jarocka-karpowicz, E. Skrzydlewskas, Antioxidative and anti-inflammatory properties of cannabidiol, Antioxidants 9 (2020) 1–20, https://doi.org/10.3390/antiox9010021.
[21] S.A. Millar, R.F. Maguire, A.S. Yates, S.E. O'Sullivan, Towards better delivery of cannabidiol (CBD), Pharm. Times 13 (2020) 219, https://doi.org/10.3390/PH13090219, 13 (2020) 219.
[22] A.I. Fraguas-Sánchez, A. Fernández-Carballido, R. Simancas-Herbada, C. Martin-Sabroso, A.I. Torres-Suárez, CBD loaded microparticles as a potential formulation to improve paclitaxel and doxorubicin-based chemotherapy in breast cancer, Int. J. Pharm. 574 (2020), 118916, https://doi.org/10.1016/j.ijpharm.2019.118916.
[23] R.A. Ross, Anandamide and vanilloid TRPV1 receptors, Br. J. Pharmacol. 140 (2003) 790–801, https://doi.org/10.1038/sj.bjp.0705467.
[24] A.I. Fraguas-Sánchez, A. Fernández-Carballido, C. Martin-Sabroso, A.I. Torres-Suárez, Stability characteristics of cannabidiol for the design of pharmacological, biochemical and pharmaceutical studies, J. Chromatogr. B 1150 (2020), 122188, https://doi.org/10.1016/J.JCHROMB.2020.122188.
[25] C. Itin, D. Barasch, A.J. Domb, A. Hoffman, Prolonged oral transmucosal delivery of highly lipophilic drug cannabidiol, Int. J. Pharm. 581 (2020), https://doi.org/10.1016/j.ijpharm.2020.119276.
[26] A.I. Fraguas-Sánchez, A.I. Torres-Suárez, M. Cohen, F. Delie, D. Bastida-Ruiz, L. Yart, C. Martin-Sabroso, A. Fernández-Carballido, PLGA nanoparticles for the intraperitoneal administration of CBD in the treatment of ovarian cancer: in vitro and in Ovo assessment, Pharmaceutics 12 (2020) 1–19, https://doi.org/10.3390/pharmaceutics12050439.
[27] P. Lv, D. Zhang, M. Guo, J. Liu, X. Chen, R. Guo, Y. Xu, Q. Zhang, Y. Liu, H. Guo, M. Yang, Structural analysis and cytotoxicity of host-guest inclusion complexes of cannabidiol with three native cyclodextrins, J. Drug Deliv. Sci. Technol. 51 (2019) 337–344, https://doi.org/10.1016/j.jddst.2019.03.015.
[28] A.P. Matarazzo, L.M.S. Elisei, F.C. Carvalho, R. Bonfílio, A.L.M. Ruela, G. Galdino, G.R. Pereira, Mucoadhesive nanostructured lipid carriers as a cannabidiol nasal delivery system for the treatment of neuropathic pain, Eur. J. Pharmaceut. Sci. 159 (2021), https://doi.org/10.1016/j.ejps.2020.105698.
[29] P. Taslimi, İ. Gulçin, Antioxidant and anticholinergic properties of olivetol, J. Food Biochem. 42 (2018), https://doi.org/10.1111/jfbc.12516.
[30] T.J. Raharjo, W. Te Chang, Y.H. Choi, A.M.G. Peltenburg-Looman, R. Verpoorte, Olivetol as product of a polyketide synthase in Cannabis sativa L, Plant Sci. 166 (2004) 381–385, https://doi.org/10.1016/J.PLANTSCI.2003.09.027.
[31] A. Brizzi, F. Aiello, S. Boccella, M.G. Cascio, L. De Petrocellis, M. Frosini, F. Gado, A. Ligresti, L. Luongo, P. Marini, C. Mugnaini, F. Pessina, F. Corelli, S. Maione, C. Manera, R.G. Pertwee, V. Di Marzo, Synthetic bioactive olivetol-related amides: the influence of the phenolic group in cannabinoid receptor activity, Bioorg. Med. Chem. 28 (2020), 115513, https://doi.org/10.1016/j.bmc.2020.115513.
[32] N. Motakef-Kazemi, S.A. Shojaosadati, A. Morsali, In situ synthesis of a drug-loaded MOF at room temperature, Microporous Mesoporous Mater. (2014), https://doi.org/10.1016/j.micromeso.2013.11.036.
[33] H. Guo, Y. Zhu, S. Wang, S. Su, L. Zhou, H. Zhang, Combining coordination modulation with acid-base adjustment for the control over size of metal-organic frameworks, Chem. Mater. 24 (2012) 444–450, https://doi.org/10.1021/cm202593h.
[34] D. Ke, J.F. Feng, D. Wu, J.B. Hou, X.Q. Zhang, B.J. Li, S. Zhang, Facile stabilization of a cyclodextrin metal-organic framework under humid environment: via hydrogen sulfide treatment, RSC Adv. 9 (2019) 18271–18276, https://doi.org/10.1039/c9ra03079d.
[35] M. Al Haydar, H.R. Abid, B. Sunderland, S. Wang, Metal organic frameworks as a drug delivery system for flurbiprofen, Drug Des. Dev. Ther. (2017), https://doi.org/10.2147/DDDT.S145716.
[36] R.S. Forgan, R.A. Smaldone, J.J. Gassensmith, H. Furukawa, D.B. Cordes, Q. Li, C. E. Wilmer, Y.Y. Botros, R.Q. Snurr, A.M.Z. Slawin, J.F. Stoddart, Nanoporous carbohydrate metal-organic frameworks, J. Am. Chem. Soc. 134 (2012) 406–417, https://doi.org/10.1021/ja208224f.
[37] I. Roy, J.F. Stoddart, Cyclodextrin metal–organic frameworks and their applications, Acc. Chem. Res. (2021), https://doi.org/10.1021/acs.accounts.0c00695.
[38] G. Zhang, F. Meng, Z. Guo, T. Guo, H. Peng, J. Xiao, B. Liu, V. Singh, S. Gui, P. York, W. Qian, L. Wu, J. Zhang, Enhanced stability of vitamin A palmitate microencapsulated by γ-cyclodextrin metal-organic frameworks, J. Microencapsul. 35 (2018) 249–258, https://doi.org/10.1080/02652048.2018.1462417.
[39] T. Dong, Y. He, K.M. Shin, Y. Inoue, Formation and characterization of inclusion complexes of poly(butylene succinate) with α- and γ-cyclodextrins, Macromol. Biosci. 4 (2004) 1084–1091, https://doi.org/10.1002/mabi.200400054.
[40] M. Wei, A.E. Tonelli, Compatibilization of polymers via coalescence from their common cyclodextrin inclusion compounds, Macromolecules 34 (2001) 4061–4065, https://doi.org/10.1021/ma010235a.
[41] Y. Xiong, L. Wu, T. Guo, C. Wang, W. Wu, Y. Tang, T. Xiong, Y. Zhou, W. Zhu, J. Zhang, Crystal transformation of β-CD-MOF facilitates loading of dimercaptosuccinic acid, AAPS PharmSciTech 20 (2019) 1–9, https://doi.org/10.1208/s12249-019-1422-z.
[42] M. Kumar Trivedi, A. Branton, Characterisation of physical, spectral and thermal properties of biofield treated resorcinol, Org. Chem. Curr. Res. (2015), https://doi.org/10.4172/2161-0401.1000146, 04.
[43] D.J. Prasad Reddy, A.V. Rajulu, V. Arumugam, M.D. Naresh, M. Muthukrishnan, Effects of resorcinol on the mechanical properties of soy protein isolate films, J. Plastic Film Sheeting 25 (2009) 221–233, https://doi.org/10.1177/8756087910365030.
[44] X. Ren, H. Cai, H. Du, J. Chang, The preparation and characterization of pyrolysis bio-oil-resorcinol-aldehyde resin cold-set adhesives for wood construction, Polymers 9 (2017), https://doi.org/10.3390/polym9060232.
[45] H. Gu, Olivetol-cyclodextrin Complexes and Regio-Selective Process for Preparing Delta 9-tetrahydrocannabinol, WO2004092101A3, 2004.
[46] Z. Moussa, M. Hmadeh, M.G. Abiad, O.H. Dib, D. Patra, Encapsulation of curcumin in cyclodextrin-metal organic frameworks: dissociation of loaded CD-MOFs enhances stability of curcumin, Food Chem. (2016), https://doi.org/10.1016/j.foodchem.2016.06.013.
[47] J.S. Choi, W.J. Son, J. Kim, W.S. Ahn, Metal–organic framework MOF-5 prepared by microwave heating: factors to be considered, Microporous Mesoporous Mater. 116 (2008) 727–731, https://doi.org/10.1016/J.MICROMESO.2008.04.033.